

1

Enhanced Artificial Neural Networks for Salinity Estimation and 2 Forecasting in the Sacramento-San Joaquin Delta of California

3 Siyu Qi¹, Zhaojun Bai², Zhi Ding³, Nimal Jayasundara⁴, Minxue He⁵, Prabhjot Sandhu⁶,
4 Sanjaya Seneviratne⁷, and Tariq Kadir⁸

5 ¹Dept. of Electrical and Computer Engineering, University of California, Davis, CA 95616
6 (Email:syqi@ucdavis.edu)

7 ²Dept. of Computer Science, University of California, Davis, CA 95616
8 (Email:bai@cs.ucdavis.edu)

9 ³Dept. of Electrical and Computer Engineering, University of California, Davis, CA 95616
10 (Email:zding@ucdavis.edu)

11 ⁴Bay Delta Office, California Dept. of Water Resources, 1416 9th St., Sacramento, CA 95614
12 (Email:nimal.jayasundara@water.ca.gov)

13 ⁵Bay Delta Office, California Dept. of Water Resources, 1416 9th St., Sacramento, CA 95614
14 (Email:kevin.he@water.ca.gov)

15 ⁶Bay Delta Office, California Dept. of Water Resources, 1416 9th St., Sacramento, CA 95614
16 (Email:prabhjot.sandhu@water.ca.gov)

17 ⁷Bay Delta Office, California Dept. of Water Resources, 1416 9th St., Sacramento, CA 95614
18 (Email:sanjaya.seneviratne@water.ca.gov)

19 ⁸Bay Delta Office, California Dept. of Water Resources, 1416 9th St., Sacramento, CA 95614
20 (Email:tariq.kadir@water.ca.gov)

21 **ABSTRACT**

22 Domain-specific architectures of artificial neural networks (ANNs) have been developed to
23 estimate salinity levels for planning at key monitoring stations in the Sacramento-San Joaquin

24 Delta (Delta), California. In this work, we propose three major enhancements to existing ANN
25 architectures for purposes of training time reduction, estimation error reduction and better feature
26 extraction. Specifically, we design a novel multi-task ANN architecture with shared hidden layers for
27 joint salinity estimation at multiple stations, achieving a reduction of 90% training and inference
28 time. As another major structural redesign, we replace pre-determined pre-processing on input
29 data by a trainable convolution layer. We further enhance the multi-task ANN design and training
30 for salinity forecasting. Test results indicate that these enhancements substantially improve the
31 efficiency and expand the capacity of the current salinity modeling ANNs in the Delta. Our enhanced
32 ANN design methodologies have the potential for incorporation into the current modeling practice
33 and provide more robust and timely information to guide water resource planning and management
34 in the Delta.

35 INTRODUCTION

36 The Sacramento-San Joaquin Delta consists of a maze of interconnected channels that are
37 central to California's water supply systems. Major streams like the Sacramento River, San Joaquin
38 River, and eastside tributaries enter the Delta (Fig. 1) and the waters flow through the Delta in a
39 complex network of intersecting channels which ultimately flow west out to the Pacific Ocean or are
40 diverted for agricultural and municipal use inside and outside of the Delta. The salinity of water in
41 the channels (concentration of salt measured, for example, in milligrams of salt per liter of stream
42 water) determines the suitability for fish and wildlife, growing crops (the Delta has approximately
43 420,000 acres of prime agricultural lands), and urban indoor/outdoor use. Water salinities in the
44 Delta channels are affected by many factors including ocean tides, inflows to the Delta from inland
45 rivers and streams, and agricultural activities/practices within the Delta. Also, human actions
46 related to water usage such as diverting to the Delta islands for Agricultural and urban use, or
47 exports from the Delta through the State Water Project (SWP) and Central Valley Project (CVP)
48 pumping plants would also change flows and salinities through the mixing process. To ensure safe
49 water use, ecosystem sustainability, and economic viability, State and federal regulatory agencies
50 have established several salinity criteria (maximum concentrations not to be exceeded) spatially

51 and temporally within the Delta. One such regulatory example is the Water Right Decision 1641
52 (D1641) of the California State Water Resources Control Board ((SWRCB) 2000) which specifies
53 the threshold salinity values at certain compliance locations during certain periods in a year. To
54 assist in the planning and management of the water resources in the Delta, the California Department
55 of Water Resources (CDWR) has developed two key simulation models for use in planning studies:
56 (1) CalSim, a water allocation model of the SWP and CVP systems (Draper et al. 2004), and (2) Delta
57 Simulation Model 2 (DSM2), a hydrodynamics and water quality model (DWR-DSM2 2019), which
58 is developed based upon the mathematical flow-salinity relationship model presented in (Denton
59 1993; Denton and Sullivan 1993). We refer interested readers to an earlier paper (Jayasundara et al.
60 2020) on detailed discussions of CalSim and DSM2 as tools used in water resource management
61 and their functionalities. There are 12 key water quality monitoring stations in the Delta: Emmaton,
62 Jersey Point, Collinsville, Rock Slough, Antioch, Mallard Island, Old River at HWY 4, Martinez,
63 Middle River Intake, Victoria Intake, CVP Intake and Clifton Court Forebay (CCFB) Intake (see
64 Fig. 1). However, computational runtimes and other programming factors limit simulations of
65 CalSim and DSM2 concurrently during a planning.

66 ANNs have been developed and applied extensively in the field of water resources engineering
67 to model (Ranjithkumar and Robert 2021; Tung et al. 2020; Tealab 2018; Kang et al. 2017), for
68 instance, groundwater level (Chen et al. 2011), surface runoff (Swain et al. 2017), reservoir opera-
69 tions (Chandramouli and Raman 2001), water demand (Bata et al. 2020), leak detection(Bohorquez
70 et al. 2020), and water system control (Hajgató et al. 2020). ANNs have also been explored in
71 modeling salinity in groundwater (Banerjee et al. 2011), soil (Dai et al. 2011; Jiang et al. 2019),
72 Oceans (Bhaskaran et al. 2010; Chen and Hu 2017), rivers (Bowden et al. 2005; Hunter et al. 2018;
73 Maier and Dandy 1999), and estuarine environments (DeSilet et al. 1992; Huang and Foo 2002;
74 Sreekanth and Datta 2010; Le et al. 2019; Zhou et al. 2020). ANNs have only been applied recently
75 in salinity modeling in the Delta (Chen et al. 2018; Rath et al. 2017; He et al. 2020; Jayasundara
76 et al. 2020). Specifically, Chen et al. (2018) proposed a one-dimensional hydrodynamic model
77 emulator to represent estuarine mixing and water quality in the northern reach of the San Francisco

78 Bay-Delta estuary, California, while Rath et al. (2017) developed an ANN-incorporated hybrid
79 model of salinity in the same estuary. He et al. (2020) investigated the use of MLP ANNs in
80 estimating boundary salinity in the Delta based on water flow and tidal stage.

81 Jayasundara et al. (2020), for the first time, have developed and applied individual MLP ANNs
82 consisting of one input layer, two hidden layers, and one output layer, in simulating salinity based
83 on seven variables in the Delta, including water control gate operations, water exports, tidal stage,
84 as well as flow and salinity boundaries, to emulate DSM2 within CalSim 3, making runtimes much
85 more practical. However, it is not efficient to train and inference those 12 separate ANNs. In the
86 context of our objective for simultaneously estimating salinity levels at multiple monitoring stations
87 based on the same set of inputs, we can view this problem as a special case of multi-task learning
88 (MTL). This formulation is motivated by the fact that the salinities at the multiple monitoring
89 stations are all affected by the same set of hydrological measurements within the same regional
90 ecosystem.

91 MTL, in contrast to single-task learning (STL), is a machine learning strategy where multiple
92 tasks sharing commonalities are solved simultaneously. As shown in (Caruana 1993; Caruana
93 1995; Ruder 2017), the domain-specific information contained in input data may allow one task to
94 “eavesdrop” on features discovered for other related tasks and may lead the model to prefer some
95 hypotheses over others. By leveraging the domain-specific information, MTL helps improve neural
96 networks’ efficacy and generalizability. One of the most commonly used MTL methods is known
97 as *hard parameter sharing*, which is achieved by a joint architecture that requires multiple tasks to
98 share some hidden layers while keeping several task-specific layers towards the end of model for each
99 task (Caruana 1993). The idea of hard parameter sharing has been applied to time series prediction
100 such as energy flux prediction (Guijo-Rubio et al. 2020), rainfall amount prediction(Qiu et al.
101 2017) and water quality forecasting(Liu et al. 2016). We design the MTL ANN for simultaneous
102 estimation of salinity at multiple monitoring stations and this new paradigm enables the ANN to
103 better extract the underlying data features and generate better overall performance than the current
104 STL model individually trained and optimized for each monitoring station (Jayasundara et al. 2020).

105 In addition, as MTL has been successfully applied to time series prediction tasks in (Guijo-Rubio
106 et al. 2020; Qiu et al. 2017; Liu et al. 2016), we test and analyze the prediction capability of our
107 proposed ANNs.

108 Generally, the current study stems from the Jayasundara et al. (2020) study but extended all
109 those previous studies in the Delta in terms of:

- 110 1. Improved ANN training efficiency by applying a joint MTL approach.
- 111 2. Exploration of ANN-based salinity forecasting efficacy for the Delta.
- 112 3. Improved ANN performance through systematic pre-processing of input time series by
113 using a trainable convolution layer.
- 114 4. Expansion of ANN to discover the relationship between performance and their size.

115 METHODS

116 Similar to the approach described in (Jayasundara et al. 2020), we aim to improve salinity
117 estimation by leveraging the seven hydrological, water quality and operation parameters, namely
118 Northern Net flows (Sacramento River and East side Streams); San Joaquin river flows; Delta
119 cross-channel gate operation; net Delta consumptive use; tidal energy; San Joaquin River inflow
120 salinity at Vernalis; SWP and CVP exports via Banks pumping plant, Jones pumping plant, and
121 Contra Costa canal (see Fig. 2). We will estimate salinities at a number of measurement points
122 which include Emmaton, Jersey Point, Collinsville and Rock Slough, among others. The input
123 data are the (pre-processed) seven input variables. Following (Jayasundara et al. 2020), each of the
124 seven variables is pre-processed via an empirical convolution process that converts the values of
125 the input at the current day plus the antecedent 117 days into 18 values, including one value from
126 each of the current day plus the most recent seven antecedent days along with 10 non-overlapping
127 11-day averages. Fig. 3 outline the pipeline to obtain the estimated salinity levels in (Jayasundara
128 et al. 2020).

129 **Network Inputs and Outputs**

130 The complete pipeline in mathematical notation is given in Fig. 4. We use subscript for matrix
 131 and vector indexing and superscript to denote the variable. For example, $x_{n,t_r}^{(m)}$ is the t_r -th value
 132 for m -th input parameter in ANN's input vector for day n . As explained in Section 1, there are
 133 seven input parameters and 12 output parameters. For training and validation, we have access to
 134 monthly input data and daily salinity data covering water years 1941-2015. In California, each water
 135 year cycle runs from October 1 to September 30 of the following calendar year. As described in
 136 (Jayasundara et al. 2020), CalSim can refine monthly data record into daily by spline interpolation.

137 There is a total of N data samples (or days) in the dataset. In our problem, we select $M = 7$
 138 observation variables. Same as in CalSim (Jayasundara et al. 2020), we pick $T = 118$ and $T_r = 18$
 139 in the baseline case and pre-process the data as denoted in Fig. 5.

140 For input variable m on day n , we extract 8 daily values:

$$141 \quad x_{n,i}^{(m)} = z_{n-i+1}^{(m)}, \quad (1)$$

142 where $i \in \{1, \dots, 8\}$. We also compute a total of 10 successive but non-overlapping 11-day moving
 143 averages before the first daily data $x_{n,i}^{(m)}$, $i \in \{1, \dots, 8\}$ to be stored in

$$144 \quad x_{n,i+8}^{(m)} = \frac{1}{11} \sum_{j=1}^{11} z_{n-11i-j+4}^{(m)}, \quad (2)$$

145 where $i \in \{1, \dots, 10\}$. Altogether, for the M variables in each day n , we form $M \times T_r = 7 \times 18 = 126$
 146 values as the $M \times T_r$ input matrix x_n to the ANNs.

147 Later for exploring a different ANN architecture to bypass this rather *ad hoc* pre-processing,
 148 we would form a trainable convolution layer instead of applying the above pre-determined pre-
 149 processing steps. In that case, those 118 daily values of each of the seven variables are directly
 150 provided to the convolution layer. The corresponding details will be described in Section 2.

151 The target outputs of ANNs are the salinity levels at one or more monitoring stations. Each STL

152 ANN's output is salinity level at one single monitoring station, while each MTL ANN's outputs
153 are salinity levels at all 12 monitoring stations.

154 Different from the previous study (Jayasundara et al. 2020), the current work randomly split
155 80% and 20% of this dataset for training and validation, respectively.

156 **Multi-Task Learning**

157 The goals of ANNs are to predict salinity at multiple monitoring stations which are physically
158 related to one another in the Delta. It is therefore natural that these ANNs can share some of the
159 same features of the underlying data inputs. To improve the ANN for individual monitoring stations
160 (Jayasundara et al. 2020), we explore the MTL approach for the 12 monitoring stations under study.

161 As described in (Caruana 1995), these inter-related multiple tasks may be learned jointly by
162 training a single ANN. The output layers shall include more neurons whereas the hidden layers
163 are shared by the monitoring stations. These hidden layers together serve as a joint mechanism
164 for feature extractions that can be used more consistently to generate salinity estimates at different
165 monitoring stations. With MTL, an ANN can show better general performance over multiple
166 disjoint single-task ANNs. As shown in Fig. 6, the MLP architecture proposed in (Jayasundara
167 et al. 2020) consists of two fully connected (FC) hidden layers and one output layer, with each layer
168 containing 8 neurons, 2 neurons and 1 neuron, respectively.

169 Based on the model in previous successful STL ANNs in Fig. 6, we build the multi-task
170 ANN architecture, which is an MLP network containing two hidden layers with sigmoid activation
171 functions and one output layer with a Leaky ReLU (Maas et al. 2013) activation function. As
172 illustrated in Fig. 7, we increase number of neurons by a factor of 12, which coincides with the
173 number of monitoring stations, for all layers to build the multi-task ANN, that is, the two hidden
174 layers and output layer in multi-task ANN contain 96, 24 and 12 neurons respectively. We also
175 explored various ANN sizes in Section "ANN Size".

176 **Trained Input Pre-processing via a Convolution Layer**

177 As discussed earlier, the authors of (Jayasundara et al. 2020) utilized 8 newest daily values
178 together with 10 non-overlapping moving averages of the daily values immediately before the 8

179 daily values as input data for salinity estimation (Fig. 5).

180 It should be recognized that the reported direct daily mappings and moving window averages
181 are special cases of convolution processing, except that the existing pre-processing is not optimized
182 through data training. Understanding the shortcomings of such a heuristic pre-processing, we
183 propose instead to include a trainable convolution layer for data pre-processing in our novel ANN
184 architecture. Mathematically, the convolution layer would implement the following data processing
185 through the training weights $f_{j,i}^{(m)}$:

$$186 \quad \mathbf{x}_{n,i}^{(m)} = \sum_{j=1}^T \mathbf{z}_{n-j+1}^{(m)} \times \mathbf{f}_{j,i}^{(m)}, \quad (3)$$

187 where $n \in \{1, \dots, N\}$, $m \in \{1, \dots, M\}$ and $i \in \{1, \dots, T_r\}$. Clearly, by appropriately setting
188 the convolution weights $f_{j,i}^{(m)}$, the convolution layer is capable of delivering daily value mapping
189 and sliding window averaging. Moreover, this convolution layer is trainable in conjunction with
190 the additional layers in the ANN. The inclusion of the convolution layer within the ANN allows
191 the weights in this layer and other ANN layers be jointly optimized to achieve better overall
192 performance.

193 By including the convolution layer, the two respective novel architectures of single-task and
194 multi-task ANNs with a convolution layer are shown in Fig. 8. There are $T_r = 18$ filters in a
195 convolution layer such that the convolution layers are able to extract at least the same 8 daily values
196 and 10 average values in the pre-determined pre-processing. The complete pipeline with proposed
197 convolution layer and the MTL ANN can be found in Fig. 9.

198 Salinity Forecasting

199 The ability to forecast salinity at key monitoring stations with lead time up to several days can
200 present an important opportunity and advantage to the water operations in the Delta. This can be
201 especially important for real-time operators of the SWP and CVP reservoirs to ensure that adequate
202 released water reaches the Delta to ensure regulatory compliance at the salinity monitoring stations;
203 for example, it takes approximately five days for water released from the Shasta reservoir (a CVP

204 facility) and three days for water released from the Lake Oroville reservoir (a SWP facility) to
205 reach the Delta. The existing ANN studies have not tackled this challenging problem. From a
206 physical point of view, the dynamics between the input hydrological parameters and the salinity level
207 measurements provide a strong motivation to suggest the possible success of salinity forecasting.
208 Successful forecasting can also provide vital insight into the development of future models.

209 In this work, we investigate and explore the proposed MTL ANN for salinity forecasting at
210 the 12 monitoring stations. We utilize the same architecture to test the performance on salinity
211 prediction tasks. In this case, with a set of inputs for day n , a MTL ANN learns to predict the
212 salinity levels \mathbf{y}_{n+i} , $i \in \{1, \dots, 7\}$ on day $n+i$.

213 Optimizer

214 In (Jayasundara et al. 2020), the authors adopt both Levenberg-Marquardt (LM) (Marquardt
215 1963; Levenberg 1944) optimization algorithm and Bayesian regularization (Foresee and Hagan
216 1997) to update weights and biases in ANNs. However, as mentioned in (Wilamowski et al. 2001),
217 the demand for large memory to compute Jacobian matrices and the need for inverting matrices
218 are the major drawbacks of the LM algorithm. When the number of trainable parameters in ANN
219 increases, the computational complexity of LM algorithm grows exponentially. In this paper, we
220 utilize one of the modern optimizers, the Adam optimizer (Kingma and Ba 2014), to train the
221 ANNs. The Adam optimizer is computationally efficient and requires little memory. As a result,
222 the Adam optimizer is well suited for machine learning problems with complex network architecture
223 (as proposed in this paper) and/or large datasets.

224 ANN Size

225 The number of hidden layers and neurons in these layers determines the number of trainable
226 parameters and the potential capability of an ANN. There is a trade-off between ANN complexity
227 and performance. Generally, performance on the training dataset usually improves with the increase
228 of the ANN size before the problem of overfitting occurs due to limited data, because a larger ANN
229 is capable of learning a more complex non-linear function. Meanwhile, as the ANN gets deeper
230 and/or wider, the probability of overfitting increases, and the computation complexity grows. To

231 find the architecture that fits this specific problem, we vary the depth and width of multi-task ANNs
 232 and observe how their performance changes on the test dataset.

233 **RESULTS AND ANALYSIS**

234 **Implementation**

235 We implement the newly developed ANNs using the popular open source library, Tensorflow
 236 2.2.0 (Abadi et al. 2015), with Python 3.6.9. We conduct the experiments through web-browser on
 237 Google Colaboratory, which is a cloud-based Jupyter notebook environment with a Tesla T4 GPU.
 238 We normalize inputs and outputs to the range [0.1, 0.9] by linearly converting the i -th daily value
 239 of the k -th input variable in the n -th data sample $\mathbf{x}_{n,i}^{(m)}$ to

$$240 \quad \widehat{\mathbf{x}}_{n,i}^{(m)} = \frac{\mathbf{x}_{n,i}^{(m)} - \left(\min_{k=1,\dots,N} \mathbf{x}_{k,i}^{(m)} \right)}{\left(\max_{k=1,\dots,N} \mathbf{x}_{k,i}^{(m)} \right) - \left(\min_{k=1,\dots,N} \mathbf{x}_{k,i}^{(m)} \right)} \times 0.8 + 0.1. \quad (4)$$

241 We apply the same normalization to outputs \mathbf{y}_n representing the salinity at a monitoring station on
 242 day n .

$$243 \quad \widehat{\mathbf{y}}_n = \frac{\mathbf{y}_n - \left(\min_{k=1,\dots,N} \mathbf{y}_k \right)}{\left(\max_{k=1,\dots,N} \mathbf{y}_k \right) - \left(\min_{k=1,\dots,N} \mathbf{y}_k \right)} \times 0.8 + 0.1. \quad (5)$$

244 The cost function used for training is the Mean Squared Error (MSE). For the LM optimizer, we
 245 adopt the same settings as (Jayasundara et al. 2020), where the starting learning rate is 0.005 and
 246 decay factor is 10 and the training takes 150 epochs. For the Adam optimizer, the learning rate
 247 is determined using a grid search. The starting learning rate is 0.01, and it is scaled by 0.1, 0.01,
 248 0.001 and 0.0005 at epochs 80, 120, 160 and 180, respectively, and the training takes 200 epochs.

249 **Experimental Results and Discussions**

250 We evaluate the performance of the newly proposed ANN models by calculating the unitless
 251 normalized mean square error (NMSE), which is computed on the normalized salinity outputs $\widehat{\mathbf{y}}_n$
 252 based on the validation dataset. We compare the performance of several ANN architectures.

253 To begin, the basic model is a 3-layer STL ANN with pre-processed input data, consisting of
254 two hidden layers and one output layer, as shown in Fig. 6. We train this baseline ANN using
255 both the LM algorithm (STL-LM) and the Adam optimizer (STL-Adam), to illustrate the effects
256 of optimizers. Both “STL-LM” and “STL-Adam” configurations are used as baseline results for
257 comparison.

258 In our proposed ANNs based on the novel MTL strategy, we consider two different architectures:
259 (a) a basic 3-layer MTL ANN with the pre-determined data pre-processing used in the baseline
260 model using the Adam optimizer (3-MTL) for training; and (b) a 4-layer MTL ANN with a replace-
261 ment of fixed data pre-processing by a trainable convolution layer. We consider two initializations
262 for the trainable convolution layer parameters: random (4-MTL-R) and using the pre-determined
263 pre-processing parameters (4-MTL-P) according to equations 1, 2 and 3.

264 Results from each of the five configurations are labeled, respectively, by “STL-LM”, “STL-
265 Adam”, “3-MTL”, “4-MTL-R”, and “4-MTL-P”. Table 1 presents the NMSE results of the five
266 different ANN configurations. Correspondingly, Table 2 evaluates their respective training and
267 inference time (complexity). From the performance comparison, we make the following observa-
268 tions.

- 269 • With pre-determined data processing, the LM algorithm outperforms the Adam optimizer
270 in training STL ANN to generate lower NMSE values than STL-Adam and 3-MTL do at
271 all study stations, as shown in Table 1. However, the LM algorithm requires 8 times longer
272 training time (complexity) when compared with both STL and MTL trained with the Adam
273 optimizer as shown in Table 2.
- 274 • Using our newly proposed MTL architectures with a trainable convolution layer, training
275 with the Adam optimizer can substantially improve the NMSE performance over STL.
276 In particular, the 4-MTL-P results are distinctly better (with smaller NMSE values) when
277 comparing with STL-Adam at all 12 stations. The 4-MTL-P scenario outperforms STL-LM
278 at 9 out of the 12 stations.
- 279 • The proposed 4-MTL architecture not only improves the salinity estimation performance in

280 providing generally lower NMSE values, but also requires much shorter training time (from
281 8.31 hours of STL-LM to 319 seconds of 4-MTL-P) as well as much faster inference (from
282 8.52 ms to 1.3 ms). Therefore, applying MTL to multi-station salinity estimation tasks can
283 clearly improve training and inference efficiency.

284 • In 4-MTL, a trainable convolution layer significantly reduces NMSE as this data processing
285 layer can learn to extract data features and adapt to wider MTL ANN architecture through
286 training. Our pre-determined initialization helps reduce the probability of being trapped in
287 a local minimum.

288 • From Table 1, Antioch, Mallard Island and Martinez are the 3 outliers in 4-MTL-P with
289 slightly higher NMSE values than their counterparts from the STL-LM scenario. The reason
290 is that stations located further west are more influenced by ocean tides of high salinity and
291 are less effected by the input flows. Indeed, we can see from Fig. 1 that all these three
292 stations are in the western part of the Delta.

293 **Further ANN Structure Considerations**

294 We further investigate the effect of the proposed MTL ANN size and depth. Given the success
295 of the 4-layer MTL ANNs, we increase its depth and width.

296 Starting with the 4-MTL-P ANN consisting of 1 convolution layer, 2 hidden layers and 1 output
297 layer, we design 10 sets of neuron partitions in the hidden layers, while output layer contains 12
298 neurons in all cases. For the 4-layer configuration, the 10 sets of neuron partitions for the two
299 hidden layers are provided in Fig. 10.

300 We further increased the number of hidden layers to the MTL ANN by one to obtain a 5-layer
301 ANN architecture (5-MTL-P) and select 9 sets of partitions for the 3 hidden layers in 5-MTL-P. In
302 another test, we add yet another hidden layer to form a 6-layer MTL ANN (6-MTL-P). We select 3
303 sets of neuron partitions for the 4 hidden layers in 6-MTL-P. The detailed neuron partitions among
304 the hidden layers are also shown in Fig. 10.

305 The NMSE results for the 4-MTL-P, 5-MTL-P and 6-MTL-P ANNs are illustrated in Fig. 11.
306 We observe that, in general, the NMSE performance improves with increasing neural network size.

307 However, for the 12 monitoring stations, deeper ANNs with more fully connected layers in both
308 5-layer and 6-layer ANNs do not necessarily outperform a 4-layer ANN, using similar number of
309 parameters. Fig. 11 also illustrates that an expanded MTL model achieves comparable performance
310 to the STL-LM baseline model for all monitoring stations.

311 **Salinity Forecasting**

312 Physically, the salinity levels at the monitoring stations are impacted by antecedent (up to
313 months) Delta inflows. Therefore, it would be probable that one can forecast the salinity levels
314 based on current and antecedent inflow data. Hence, in addition to the same day salinity estimation
315 results obtained thus far, we further explore the efficacy of our ANN model for salinity forecasting
316 days ahead in time at the monitoring stations.

317 To investigate the prediction accuracy of our proposed 4-MTL ANN, we train seven forecasting
318 models based on the 4-MTL-P architecture as in Fig. ???. The implementation is similar to the
319 salinity estimation model and is very simple. We apply the same MTL ANN architectures except
320 that their training is based on the forecasting error. Specifically, to train a MTL ANN to forecast
321 salinity levels by i day(s), we simply train the ANN model by using the same input measurement
322 data but by advancing the output salinity level by i day(s) when calculating the MSE cost function.
323 Changing the same simple training model by advancing the output measurement by i day(s) for
324 $i = 1, \dots, 7$, we can test the efficacy of an i -day forecasting model.

325 The best experimental results are obtained using the 4-MTL-P configuration. The forecasting
326 results from 4-MTL-P are depicted in Fig. 12 as we vary $i = 0, 1, \dots, 7$ using the red line.
327 The baseline $i = 0$ estimation results from 4-MTL-P is also highlighted as a blue dashed line for
328 comparison. From the results, we make the following observations respecting the forecasting ANN.

329 • Our 4-MTL-P ANN forecasting tends to show more accurate forecasting in short term,
330 typically in 1-day or 2-day forecasting. Such result implies that there is a decent correlation
331 between upstream inflows and Delta salinity up to two days. After that, the correlation
332 tends to weaken. This is most likely because of physical distance between where flows are

333 measured and salinity monitoring stations.

334

- 335 In most cases with the exception of Emmaton, the NMSE values of forecasts with lead time
336 one day are smaller than or fairly close to their corresponding counterparts of the same
337 day salinity estimation. Emmaton differs from other stations in that it is located on the
338 Sacramento River which has significantly high runoff than other rivers (e.g., San Joaquin
339 river and eastern tributaries). The lasting impacts of flow on salinity in the Sacramento
River is not as obvious as those on other rivers.

340 **Adaptive Estimation and Forecasting Models**

341 Our test results suggest a novel adaptive hybrid ANN model in which the forecasting objectives
342 can be set uniquely for different monitoring stations, according to their physical response times. In
343 other words, depending on the geophysical distance between input and output locations, the training
344 objective function should consist of forecasting errors defined with different forecasting lead times
345 for different monitoring stations.

346 Such an adaptive ANN model can be fully incorporated within the proposed MTL framework.
347 In fact, the only adaptive parameters that we need to adjust are the lead times used in the MSE
348 cost function when training the ANN. Based on the results in Fig. 12, for each monitoring station
349 location, we vary the number of days to forecast based on their base forecasting performance.
350 With the 4-MTL-P ANN architecture as defined in Fig. ??, we manually initialize the convolution
351 filters in an ANN model during training to estimate salinity at Emmaton and forecast the remaining
352 11 stations. The final test results of the adaptive hybrid ANN model are given in Table 3. As
353 expected, 8 of the 12 monitoring stations achieved improved performance. The sum NMSE of all
354 12 monitoring stations is also lower than the pure estimation.

355 It would be natural to adjust the forecasting lead times for different monitoring stations to drive
356 down the sum NMSE further. Such fine-tuning would require a large number of experiments but
357 do not change the basic principles and the contributions of our work reported here.

358 **DISCUSSIONS AND CONCLUSIONS**

359 **Implications**

360 This study has both scientific and practical implications. From a scientific standpoint, we
361 propose the following outcomes:

362 1. The study introduces the concept of MTL into salinity modeling via ANNs in the Delta
363 for the first time. This enables estimation of salinity at multiple locations in a single
364 ANN model, with no need to develop different STL ANNs for different locations as in
365 (Jayasundara et al. 2020).

366 2. In addition, this study is the first to examine and demonstrate the capability of ANNs in
367 salinity forecasting in the Delta. This lays the foundation for further methodical exploration
368 on this front.

369 3. This study proposes a novel way of pre-processing ANN input data via a trainable convolu-
370 tion layer. Compared to the current empirical pre-processing method in (Jayasundara et al.
371 2020), this new method is modular and thus portable to additional input data.

372 Those scientific advances are not only applicable in modeling salinity, but also other important
373 environmental variables in the Delta including turbidity, dissolved oxygen concentration, water
374 temperature, among others. Additionally, their potential applications are not only limited to the
375 Delta area, but also to other estuarine environments worldwide.

376 Meanwhile, from a practical point of view, we present the following implications:

377 1. The study indicates that the MTL-based ANN proposed in this study is much more efficient
378 compared to the traditional STL-based ANNs in terms of training time and inference time
379 (Table 2). This is particularly appealing to CDWR's current modeling practice in water
380 resources planning studies. In a specific planning scenario, the current modeling practice
381 involves a process of iteratively running the planning model and the salinity emulator (i.e.,
382 current ANNs) till all salinity compliance objectives are met. Using a faster emulator
383 instead is expected to expedite the modeling process and allows more inclusive planning
384 scenarios to be assessed.

385 2. The study exemplifies the feasibility applying the proposed ANNs in salinity forecasting. In
386 practice, DSM2 is routinely utilized in forecasting salinity in the Delta to inform decision-
387 making. The proposed ANNs have the potential to supplement the current forecasting
388 practice for that purpose.

389 **Future Work**

390 This study indicates that the proposed MTL-based ANN outperforms the current STL-based
391 ANNs in most cases (Table 1). However, for three stations in western Delta (Martinez, Mallard
392 Island and Antioch), the STL-based ANNs yield slightly better estimation. We attribute the
393 probable cause to that the tide plays a more important role than upstream freshwater inflows at
394 these stations. Currently, the tidal energy (the difference between daily maximum and minimum
395 stages at Martinez) serves as the proxy for tidal impact in the input data. However, it is not a direct
396 measurement of the salinity level. As illustrated previously (He et al. 2020), sea level at the Golden
397 Gate Bridge (the downstream end of the Bay-Delta Estuary in Figure 1) is a better surrogate for
398 the salinity source of the Delta. It is also shown that incorporating sea level as an additional input
399 feature to ANNs can improve salinity estimation at Martinez (He et al. 2020). One potential future
400 enhancement to the proposed ANN is to incorporate sea level at the Golden Gate Bridge as an
401 additional input.

402 The study also shows that the forecasting skill of the proposed ANN decreases with increasing
403 lead time (Fig. 12). This is expected as the lasting influence of current day's input data (predictors)
404 on salinity (predictand) becomes weaker further into the future. To improve forecasting skills,
405 forecasted input information (e.g., forecasts on flows, tidal energy, and gate operations) can be
406 applied to drive the proposed ANN. This is a potential future direction to be explored.

407 Additionally, the ANNs examined in the current study use input data in the past 118 days since
408 salinity relates to antecedent (up to months) flows in the Delta. The deep learning architecture Long
409 Short-Term Memory (LSTM) architecture has shown special potential in simulating variables with
410 such a long memory with their predictors (He et al. 2020). This type of deep learning networks
411 will be considered in our future work.

412 Finally, this study showcases the success of applying proposed ANNs in salinity modeling in
413 the Delta. There are a wide range of other variables (e.g., precipitation, runoff volume, snow melt,
414 river stage, water temperature, turbidity) elsewhere that are critical to water resources planning
415 and management practices. The ANNs developed in the current study can be readily adapted to
416 simulate or forecast those variables in the future.

417 **Concluding Remarks**

418 This study develops enhancements to the Delta salinity modeling ANNs for the purposes of
419 training time reduction, estimation error reduction, and better feature extraction. The enhancements
420 include structural redesign on two fronts: 1) incorporation of the MTL architecture and 2) addition
421 of a convolution layer in input data pre-processing. The updated ANNs are further adapted to
422 conduct salinity forecasting which is rarely investigated previously. The enhanced ANNs have the
423 potential to be incorporated into the current modeling practice and provide more robust and timely
424 information to guide water resources planning and management in the Delta.

425 **DATA AVAILABILITY STATEMENTS**

426 The following code and data that support the findings of this study are available from the
427 corresponding author by request: Python code for training and evaluating the ANNs; input and
428 output data used in ANN training and evaluation.

429 **ACKNOWLEDGMENTS**

430 This work was supported in part by the research agreement 4600013184 from the California
431 Department of Water Resources. The views and opinions expressed in this article are those of the
432 authors and do not reflect the policy or position of their employers.

433 **NOTATIONS**

434 The following symbols are used in this paper:

M = Number of input hydrological variables denoted in Fig. 2.

N = Number of data samples, or days, in dataset.

T = Number of days' data used for estimation.

T_r = Dimension of data after pre-processing.

z_n = Time series used for estimating salinity level on day n , size is $\mathbb{R}^{M \times T}$.

x_n = Pre-processed time series with size $\mathbb{R}^{M \times T_r}$ for day n .

y_n = ANN-estimated salinity level for one or more locations on day n .

435

REFERENCES

436 Abadi, M., Agarwal, A., Barham, P., Brevdo, E., Chen, Z., Citro, C., Corrado, G. S., Davis,
437 A., Dean, J., Devin, M., Ghemawat, S., Goodfellow, I., Harp, A., Irving, G., Isard, M., Jia,
438 Y., Jozefowicz, R., Kaiser, L., Kudlur, M., Levenberg, J., Mané, D., Monga, R., Moore, S.,
439 Murray, D., Olah, C., Schuster, M., Shlens, J., Steiner, B., Sutskever, I., Talwar, K., Tucker, P.,
440 Vanhoucke, V., Vasudevan, V., Viégas, F., Vinyals, O., Warden, P., Wattenberg, M., Wicke, M.,
441 Yu, Y., and Zheng, X. (2015). "TensorFlow: Large-scale machine learning on heterogeneous
442 systems, <<https://www.tensorflow.org/>>. Software available from tensorflow.org.

443 Banerjee, P., Singh, V., Chattpadhyay, K., Chandra, P., and Singh, B. (2011). "Artificial neu-
444 ral network model as a potential alternative for groundwater salinity forecasting." *Journal of*
445 *Hydrology*, 398(3-4), 212–220.

446 Bata, M. H., Carriveau, R., and Ting, D. S.-K. (2020). "Short-term water demand forecasting using
447 nonlinear autoregressive artificial neural networks." *Journal of Water Resources Planning and*
448 *Management*, 146(3), 04020008.

449 Bhaskaran, P. K., Kumar, R. R., Barman, R., and Muthalagu, R. (2010). "A new approach for
450 deriving temperature and salinity fields in the indian ocean using artificial neural networks."
451 *Journal of marine science and technology*, 15(2), 160–175.

452 Bohorquez, J., Alexander, B., Simpson, A. R., and Lambert, M. F. (2020). “Leak detection and
453 topology identification in pipelines using fluid transients and artificial neural networks.” *Journal*
454 *of Water Resources Planning and Management*, 146(6), 04020040.

455 Bowden, G. J., Maier, H. R., and Dandy, G. C. (2005). “Input determination for neural network
456 models in water resources applications. part 2. case study: forecasting salinity in a river.” *Journal*
457 *of Hydrology*, 301(1-4), 93–107.

458 Caruana, R. (1995). “Learning many related tasks at the same time with backpropagation.” *Advances*
459 *in neural information processing systems*, 657–664.

460 Caruana, R. A. (1993). “Multitask connectionist learning.” *In Proceedings of the 1993 Connectionist*
461 *Models Summer School*, Citeseer.

462 Chandramouli, V. and Raman, H. (2001). “Multireservoir modeling with dynamic programming
463 and neural networks.” *Journal of Water Resources Planning and Management*, 127(2), 89–98.

464 Chen, L., Roy, S. B., and Hutton, P. H. (2018). “Emulation of a process-based estuarine hydrody-
465 namic model.” *Hydrological Sciences Journal*, 63(5), 783–802.

466 Chen, L.-H., Chen, C.-T., and Lin, D.-W. (2011). “Application of integrated back-propagation
467 network and self-organizing map for groundwater level forecasting.” *Journal of Water Resources*
468 *Planning and Management*, 137(4), 352–365.

469 Chen, S. and Hu, C. (2017). “Estimating sea surface salinity in the northern gulf of mexico from
470 satellite ocean color measurements.” *Remote sensing of environment*, 201, 115–132.

471 Dai, X., Huo, Z., and Wang, H. (2011). “Simulation for response of crop yield to soil moisture and
472 salinity with artificial neural network.” *Field Crops Research*, 121(3), 441–449.

473 Denton, R. and Sullivan, G. (1993). “Antecedent flow-salinity relations: Application to delta
474 planning models.” *Contra Costa Water District. Concord, California*.

475 Denton, R. A. (1993). “Accounting for antecedent conditions in seawater intrusion model-
476 ing—applications for the san francisco bay-delta.” *Hydraulic Engineering*, ASCE, 448–453.

477 DeSilet, L., Golden, B., Wang, Q., and Kumar, R. (1992). “Predicting salinity in the chesapeake
478 bay using backpropagation.” *Computers & Operations Research*, 19(3-4), 277–285.

479 Draper, A. J., Munevar, A., Arora, S. K., Reyes, E., Parker, N. L., Chung, F. I., and Peterson, L. E.
480 (2004). “CalSim: Generalized model for reservoir system analysis.” *Journal of Water Resources*
481 *Planning and Management*, 130(6), 480–489.

482 DWR-DSM2 (2019). “DSM2: Delta Simulation Model II.” *Bay Delta Office, California Dept. of*
483 *Water Resources, Sacramento, CA.*, <<https://water.ca.gov/Library/Modeling-and-Analysis/Bay-Delta-Region-models-and-tools/Delta-Simulation-Model-II>>.

485 Foresee, F. D. and Hagan, M. T. (1997). “Gauss-Newton approximation to Bayesian learning.”
486 *Proceedings of International Conference on Neural Networks (ICNN'97)*, Vol. 3, IEEE, 1930–
487 1935.

488 Guijo-Rubio, D., Gómez-Orellana, A. M., Gutiérrez, P. A., and Hervás-Martínez, C. (2020). “Short-
489 and long-term energy flux prediction using multi-task evolutionary artificial neural networks.”
490 *Ocean Engineering*, 216, 108089.

491 Hajgató, G., Paál, G., and Gyires-Tóth, B. (2020). “Deep reinforcement learning for real-time
492 optimization of pumps in water distribution systems.” *Journal of Water Resources Planning and*
493 *Management*, 146(11), 04020079.

494 He, M., Zhong, L., Sandhu, P., and Zhou, Y. (2020). “Emulation of a process-based salinity
495 generator for the sacramento–san joaquin delta of california via deep learning.” *Water*, 12(8),
496 2088.

497 Huang, W. and Foo, S. (2002). “Neural network modeling of salinity variation in apalachicola
498 river.” *Water Research*, 36(1), 356–362.

499 Hunter, J. M., Maier, H. R., Gibbs, M. S., Foale, E. R., Grosvenor, N. A., Harders, N. P., and
500 Kikuchi-Miller, T. C. (2018). “Framework for developing hybrid process-driven, artificial neural
501 network and regression models for salinity prediction in river systems.” *Hydrology and Earth*
502 *System Sciences*, 22(5), 2987–3006.

503 Jayasundara, N. C., Seneviratne, S. A., Reyes, E., and Chung, F. I. (2020). “Artificial neural network
504 for Sacramento–San Joaquin Delta flow–salinity relationship for CalSim 3.0.” *Journal of Water*
505 *Resources Planning and Management*, 146(4), 04020015.

506 Jiang, H., Rusuli, Y., Amuti, T., and He, Q. (2019). “Quantitative assessment of soil salinity
507 using multi-source remote sensing data based on the support vector machine and artificial neural
508 network.” *International journal of remote sensing*, 40(1), 284–306.

509 Kang, G., Gao, J. Z., and Xie, G. (2017). “Data-driven water quality analysis and prediction:
510 A survey.” *2017 IEEE Third International Conference on Big Data Computing Service and*
511 *Applications (BigDataService)*, IEEE, 224–232.

512 Kingma, D. P. and Ba, J. (2014). “Adam: A method for stochastic optimization.” *arXiv preprint*
513 *arXiv:1412.6980*.

514 Le, D., Huang, W., and Johnson, E. (2019). “Neural network modeling of monthly salinity variations
515 in oyster reef in apalachicola bay in response to freshwater inflow and winds.” *Neural Computing*
516 *and Applications*, 31(10), 6249–6259.

517 Levenberg, K. (1944). “A method for the solution of certain non-linear problems in least squares.”
518 *Quarterly of applied mathematics*, 2(2), 164–168.

519 Liu, Y., Liang, Y., Liu, S., Rosenblum, D. S., and Zheng, Y. (2016). “Predicting urban water quality
520 with ubiquitous data.” *arXiv preprint arXiv:1610.09462*.

521 Maas, A. L., Hannun, A. Y., and Ng, A. Y. (2013). “Rectifier nonlinearities improve neural network
522 acoustic models.” *Proc. icml*, Vol. 30, 3.

523 Maier, H. R. and Dandy, G. C. (1999). “Empirical comparison of various methods for training feed-
524 forward neural networks for salinity forecasting.” *Water Resources Research*, 35(8), 2591–2596.

525 Marquardt, D. W. (1963). “An algorithm for least-squares estimation of nonlinear parameters.”
526 *Journal of the society for Industrial and Applied Mathematics*, 11(2), 431–441.

527 Qiu, M., Zhao, P., Zhang, K., Huang, J., Shi, X., Wang, X., and Chu, W. (2017). “A short-
528 term rainfall prediction model using multi-task convolutional neural networks.” *2017 IEEE*
529 *International Conference on Data Mining (ICDM)*, IEEE, 395–404.

530 Ranjithkumar, M. and Robert, L. (2021). “Machine learning techniques and cloud computing to es-
531 timate river water quality—survey.” *Inventive Communication and Computational Technologies*,
532 Springer, 387–396.

533 Rath, J. S., Hutton, P. H., Chen, L., and Roy, S. B. (2017). “A hybrid empirical-Bayesian artifi-
534 cial neural network model of salinity in the San Francisco Bay-Delta estuary.” *Environmental*
535 *Modelling & Software*, 93, 193–208.

536 Ruder, S. (2017). “An overview of multi-task learning in deep neural networks.” *arXiv preprint*
537 *arXiv:1706.05098*.

538 Sreekanth, J. and Datta, B. (2010). “Multi-objective management of saltwater intrusion in coastal
539 aquifers using genetic programming and modular neural network based surrogate models.”
540 *Journal of Hydrology*, 393(3-4), 245–256.

541 Swain, E. D., Gómez-Fragoso, J., and Torres-Gonzalez, S. (2017). “Projecting impacts of cli-
542 mate change on water availability using artificial neural network techniques.” *Journal of Water*
543 *Resources Planning and Management*, 143(12), 04017068.

544 (SWRCB), S. W. R. C. B. (2000). “Revised water right decision 1641.

545 Tealab, A. (2018). “Time series forecasting using artificial neural networks methodologies: A
546 systematic review.” *Future Computing and Informatics Journal*, 3(2), 334–340.

547 Tung, T. M., Yaseen, Z. M., et al. (2020). “A survey on river water quality modelling using artificial
548 intelligence models: 2000–2020.” *Journal of Hydrology*, 585, 124670.

549 Wilamowski, B. M., Iplikci, S., Kaynak, O., and Efe, M. O. (2001). “An algorithm for fast
550 convergence in training neural networks.” *IJCNN’01. International Joint Conference on Neural*
551 *Networks. Proceedings (Cat. No. 01CH37222)*, Vol. 3, Ieee, 1778–1782.

552 Zhou, F., Liu, B., and Duan, K. (2020). “Coupling wavelet transform and artificial neural network
553 for forecasting estuarine salinity.” *Journal of Hydrology*, 588, 125127.

554

List of Tables

555

1	Resulting NMSE $\times 10^4$ of different ANN architectures for salinity estimation. Both inputs and outputs of ANNs are normalized.	24
2	Training time and inference time of different ANN architectures	25
3	Resulting NMSE $\times 10^4$ of 4-MTL-P ANNs for salinity estimation with/without forecasting, numbers in parentheses represent the forecast time in days for that station.	26

556

557

558

559

TABLE 1. Resulting NMSE $\times 10^4$ of different ANN architectures for salinity estimation. Both inputs and outputs of ANNs are normalized.

	STL-LM (baseline)	STL-Adam (baseline)	3-MTL	4-MTL-R	4-MTL-P
Optimizer	LM	Adam	Adam	Adam	Adam
Emmaton	3.2	9.03	10.03	4.25	2.63
Jersey Point	5.35	14.78	16.18	5.74	3.28
Collinsville	5.09	15.92	15.56	6.20	3.86
Rock Slough	5.34	13.33	17.95	6.55	3.69
Antioch	1.84	7.85	9.73	3.50	2.60
Mallard Island	2.18	8.25	9.59	3.28	2.68
Old River at HWY 4	5.01	18.99	21.03	5.27	2.71
Martinez	0.61	3.15	6.66	2.53	1.63
Middle River Intake	5.21	16.71	17.72	5.20	2.66
Victoria Intake	6.12	15.41	16.47	5.33	2.88
CVP Intake	5.11	21.32	18.95	6.97	3.94
CCFB Intake Gate	5.64	20.57	19.38	6.23	3.32

TABLE 2. Training time and inference time of different ANN architectures

Model Information	Architecture		
	STL-LM	STL-Adam	4-MTL-P
Number of parameters	981	981	16962
Optimizer	LM	Adam	Adam
Training time (sec. per model)	2493	315	319
Inference time (ms. per sample)	0.71	0.71	1.3
Number of models needed	12	12	1
Total training time	8.31 hrs	1.05 hrs	319 secs
Total inference time for all 12 stations (ms. per day)	8.52	8.52	1.3

TABLE 3. Resulting NMSE $\times 10^4$ of 4-MTL-P ANNs for salinity estimation with/without forecasting, numbers in parentheses represent the forecast time in days for that station.

Monitoring Station	Estimation only	Joint estimation and forecast
Emmaton	2.63 (0)	2.69 (0)
Jersey Point	3.28 (0)	3.25 (1)
Collinsville	3.86 (0)	3.94 (1)
Rock Slough	3.69 (0)	3.52 (1)
Antioch	2.60 (0)	2.68 (2)
Mallard Island	2.68 (0)	2.65 (1)
Old River at HWY 4	2.71 (0)	2.68 (1)
Martinez	1.63 (0)	1.54 (1)
Middle River Intake	2.66 (0)	2.65 (1)
Victoria Intake	2.88 (0)	2.79 (2)
CVP Intake	3.94 (0)	3.90 (1)
CCFB Intake Gate	3.32 (0)	3.34 (1)
Total	35.87	35.64

560 **List of Figures**

561 1	Locations of the 12 Study Salinity Stations in the San Francisco Bay and Sacramento- 562 San Joaquin Delta Estuary (Bay-Delta Estuary). The insert map shows the location 563 of the Bay-Delta Estuary in California. (Sources: Esri, DeLorme, HERE, Tom- 564 Tom, Intermap, increment P Corp., GEBCO, USGS, FAO, NPS, NRCAN, GeoBase, 565 IGN, Kadaster NL, Ordnance Survey, Esri Japan, METI, Esri China (Hong Kong), 566 swisstopo, MapmyIndia, and the GIS User Community; Data from ((SWRCB) 2000).)	28
567 2	ANN inputs and input locations. (Sources: Esri, DeLorme, HERE, TomTom, 568 Intermap, increment P Corp., GEBCO, USGS, FAO, NPS, NRCAN, GeoBase, 569 IGN, Kadaster NL, Ordnance Survey, Esri Japan, METI, Esri China (Hong Kong), 570 swisstopo, MapmyIndia, and the GIS User Community; Data from ((SWRCB) 2000).)	29
571 3	Complete pipeline for ANNs according to (Jayasundara et al. 2020)	30
572 4	Pipeline for ANNs with mathematical notations according to (Jayasundara et al. 573 2020)	31
574 5	Pre-processing diagram	32
575 6	Architecture of a single-task ANN	33
576 7	Architecture of a multi-task learning ANN	34
577 8	STL (left) and MTL (right) ANN architectures with a convolution layer.	35
578 9	Complete pipeline for proposed MTL ANNs	36
579 10	Numbers of neurons for expanded ANNs. Activation functions are not included in 580 the diagrams.	37
581 11	NMSE values for 12 monitoring stations versus number of parameters in three 582 MTL ANNs with different layers. Red dashed lines mark NMSE obtained by the 583 STL-LM baseline in Table 1.	38
584 12	NMSE values for 12 monitoring stations versus lead time (in days) with a 4-MTL-P 585 ANN. Blue dashed lines mark NMSE obtained by the 4-MTL-P case in Table 1.	39

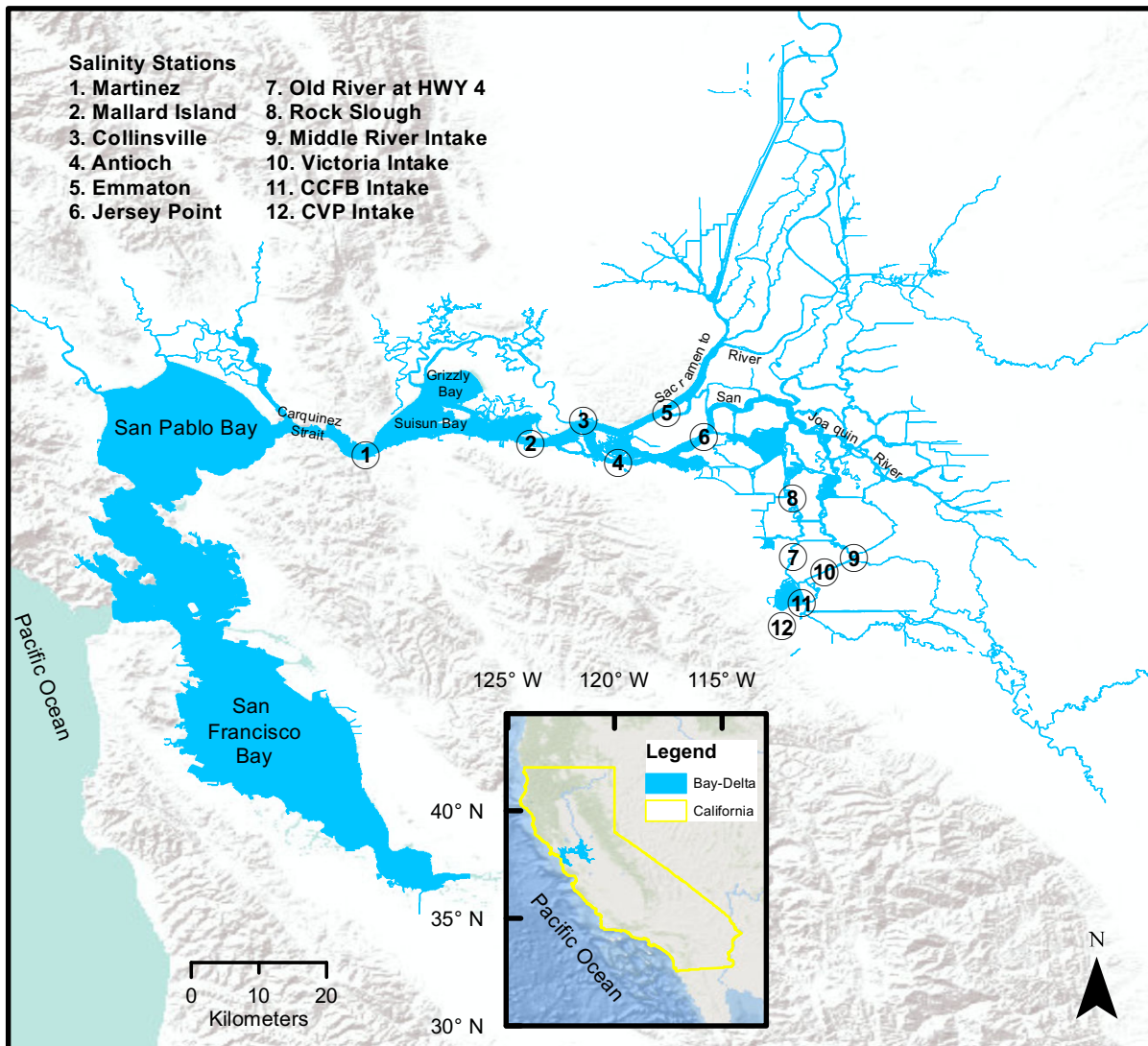


Fig. 1. Locations of the 12 Study Salinity Stations in the San Francisco Bay and Sacramento-San Joaquin Delta Estuary (Bay-Delta Estuary). The insert map shows the location of the Bay-Delta Estuary in California. (Sources: Esri, DeLorme, HERE, TomTom, Intermap, increment P Corp., GEBCO, USGS, FAO, NPS, NRCAN, GeoBase, IGN, Kadaster NL, Ordnance Survey, Esri Japan, METI, Esri China (Hong Kong), swisstopo, MapmyIndia, and the GIS User Community; Data from ([SWRCB](#)) 2000.)

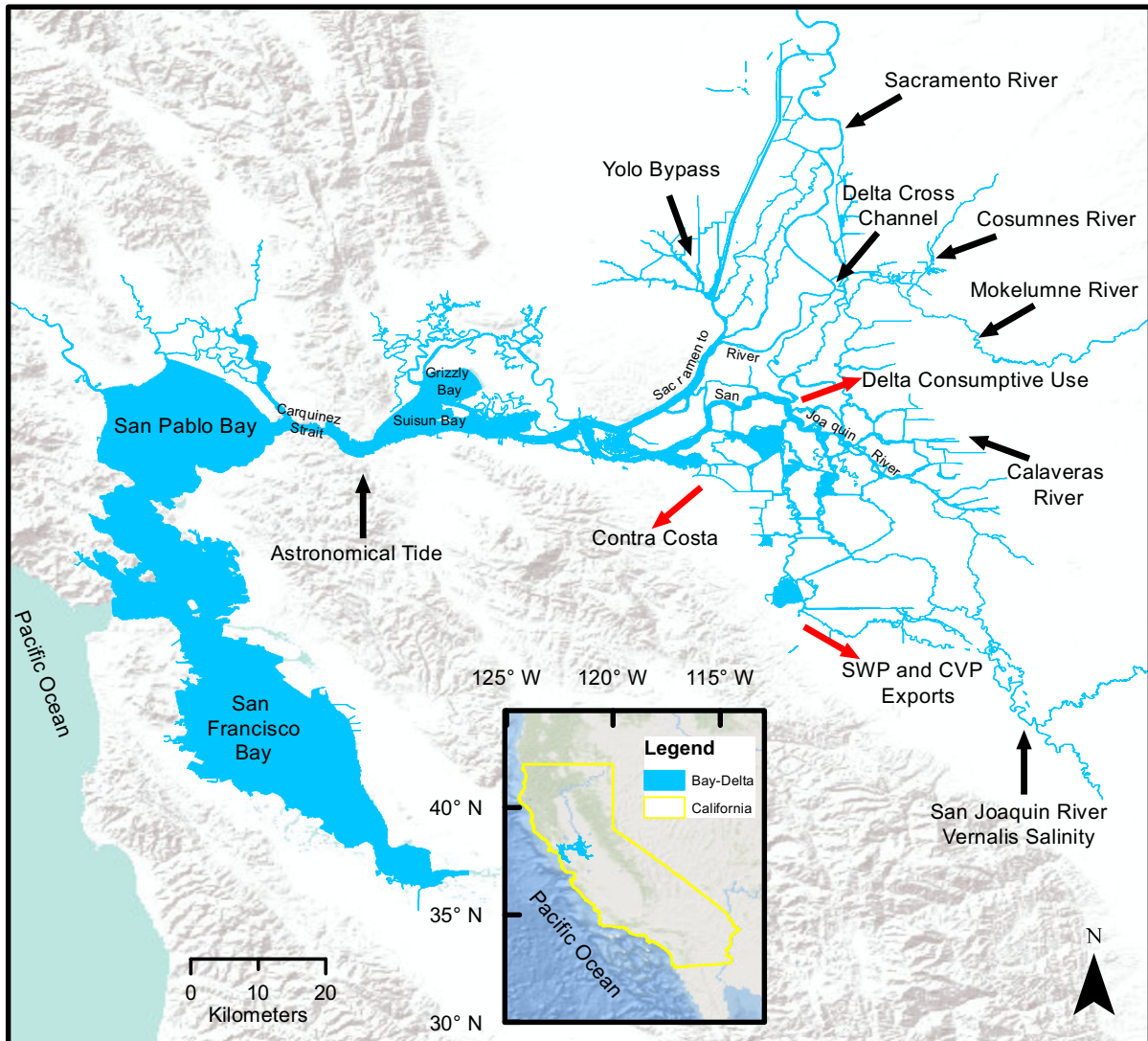


Fig. 2. ANN inputs and input locations. (Sources: Esri, DeLorme, HERE, TomTom, Intermap, increment P Corp., GEBCO, USGS, FAO, NPS, NRCAN, GeoBase, IGN, Kadaster NL, Ordnance Survey, Esri Japan, METI, Esri China (Hong Kong), swisstopo, MapmyIndia, and the GIS User Community; Data from [\(\(SWRCB\) 2000\)](#).)

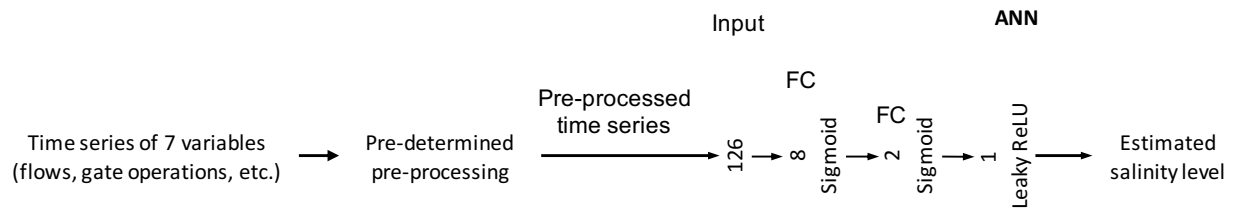


Fig. 3. Complete pipeline for ANNs according to (Jayasundara et al. 2020)

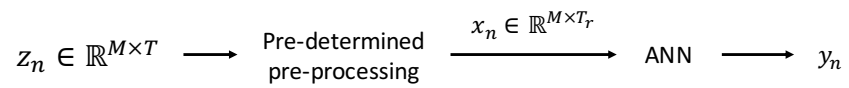


Fig. 4. Pipeline for ANNs with mathematical notations according to (Jayasundara et al. 2020)

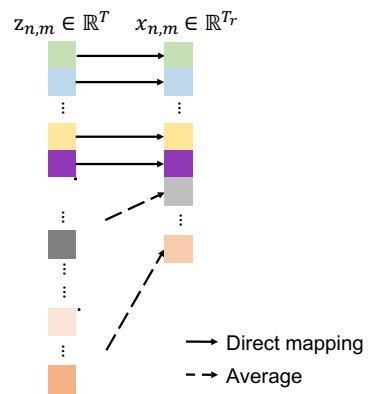


Fig. 5. Pre-processing diagram

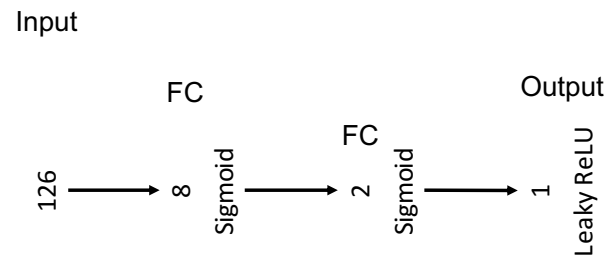


Fig. 6. Architecture of a single-task ANN

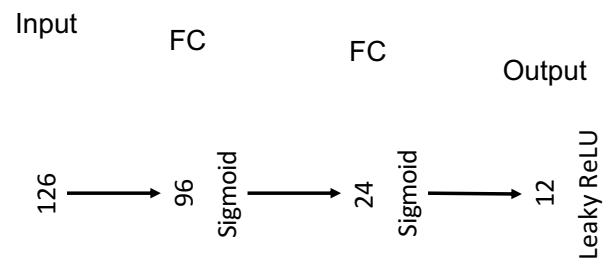


Fig. 7. Architecture of a multi-task learning ANN

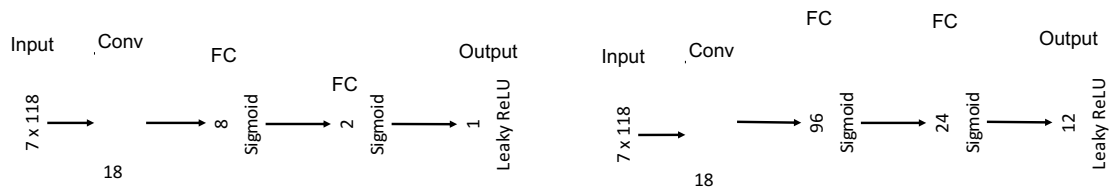


Fig. 8. STL (left) and MTL (right) ANN architectures with a convolution layer.

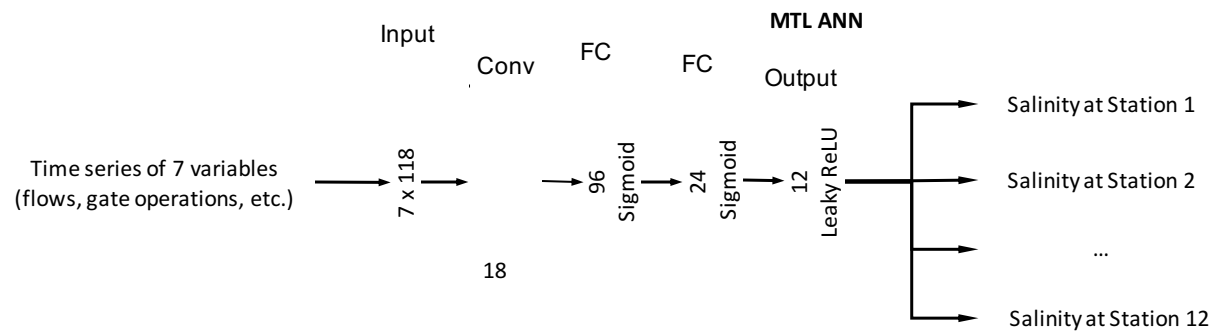


Fig. 9. Complete pipeline for proposed MTL ANNs

ANN Depth (Including Conv Layer)	Numbers of Neurons in hidden layers	Diagram
4 Layers	$n_1 = 96, n_2 = 24$	
	$n_1 = 96, n_2 = 48$	
	$n_1 = 126, n_2 = 48$	
	$n_1 = 192, n_2 = 24$	
	$n_1 = 192, n_2 = 48$	
	$n_1 = 192, n_2 = 96$	
	$n_1 = 384, n_2 = 24$	
	$n_1 = 384, n_2 = 48$	
	$n_1 = 384, n_2 = 96$	
5 Layers	$n_1 = 384, n_2 = 192$	
	$n_1 = 96, n_2 = 48, n_3 = 24$	
	$n_1 = 192, n_2 = 96, n_3 = 24$	
	$n_1 = 192, n_2 = 96, n_3 = 48$	
	$n_1 = 384, n_2 = 48, n_3 = 24$	
	$n_1 = 384, n_2 = 96, n_3 = 24$	
	$n_1 = 384, n_2 = 96, n_3 = 48$	
	$n_1 = 384, n_2 = 192, n_3 = 24$	
	$n_1 = 384, n_2 = 192, n_3 = 48$	
6 Layers	$n_1 = 384, n_2 = 192, n_3 = 96, n_4 = 48$	
	$n_1 = 192, n_2 = 96, n_3 = 48, n_4 = 24$	
	$n_1 = 384, n_2 = 192, n_3 = 96, n_4 = 24$	

Fig. 10. Numbers of neurons for expanded ANNs. Activation functions are not included in the diagrams.

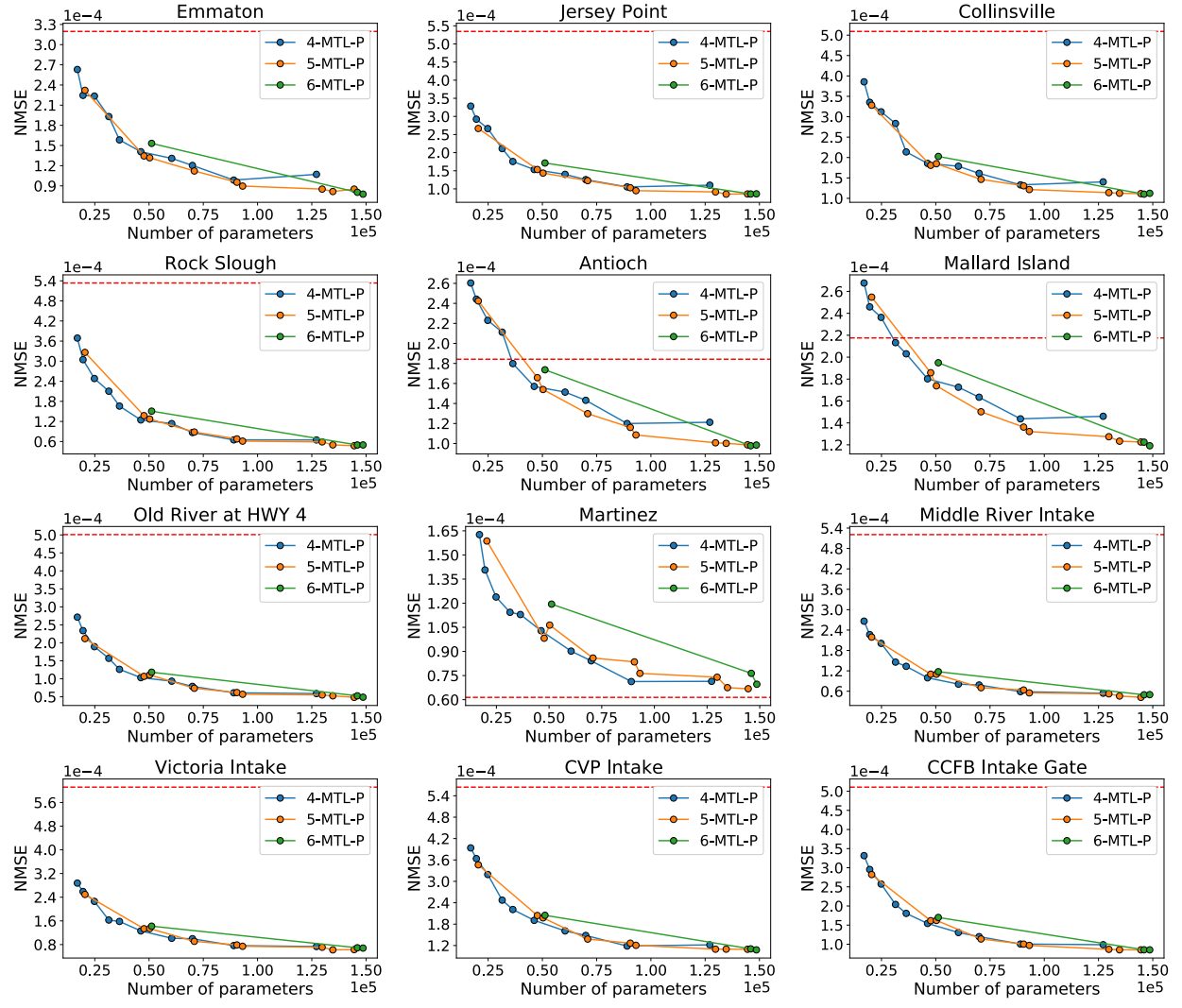


Fig. 11. NMSE values for 12 monitoring stations versus number of parameters in three MTL ANNs with different layers. Red dashed lines mark NMSE obtained by the STL-LM baseline in Table 1.

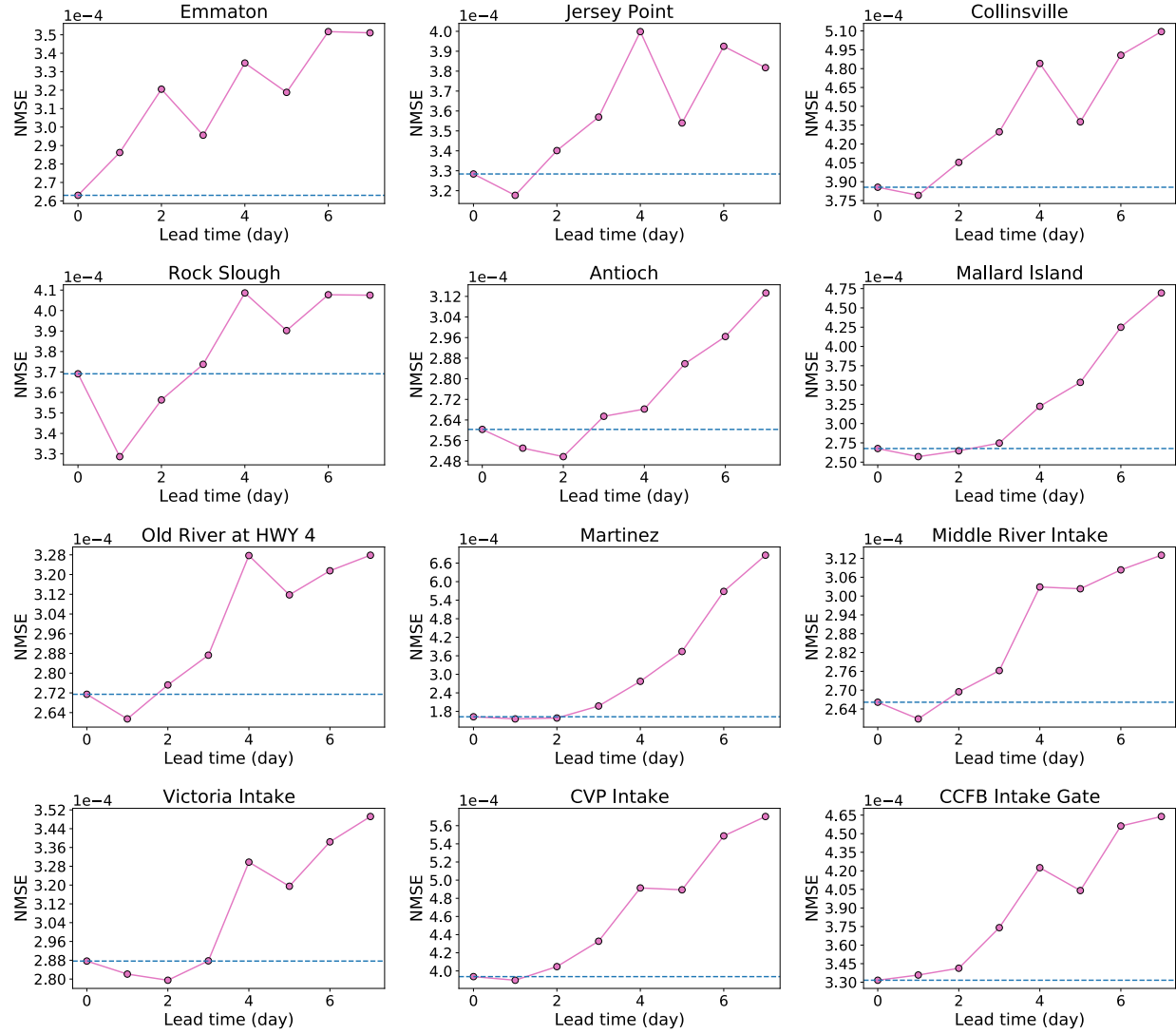


Fig. 12. NMSE values for 12 monitoring stations versus lead time (in days) with a 4-MTL-P ANN. Blue dashed lines mark NMSE obtained by the 4-MTL-P case in Table 1.